

Dalton Transactions

Accepted Manuscript



This is an *Accepted Manuscript*, which has been through the Royal Society of Chemistry peer review process and has been accepted for publication.

Accepted Manuscripts are published online shortly after acceptance, before technical editing, formatting and proof reading. Using this free service, authors can make their results available to the community, in citable form, before we publish the edited article. We will replace this *Accepted Manuscript* with the edited and formatted *Advance Article* as soon as it is available.

You can find more information about *Accepted Manuscripts* in the [Information for Authors](#).

Please note that technical editing may introduce minor changes to the text and/or graphics, which may alter content. The journal's standard [Terms & Conditions](#) and the [Ethical guidelines](#) still apply. In no event shall the Royal Society of Chemistry be held responsible for any errors or omissions in this *Accepted Manuscript* or any consequences arising from the use of any information it contains.

Cite this: DOI: 10.1039/c0xx00000x

www.rsc.org/xxxxxx

ARTICLE TYPE

Challenges in the synthetic routes to Mn(BH₄)₂: Insight into intermediate compounds

Nikolay A. Tumanov,^a Damir A. Safin,^a Bo Richter,^b Zbigniew Łodziana,^c Torben R. Jensen,^b Yann Garcia^a and Yaroslav Filinchuk^{*a}

⁵ Received (in XXX, XXX) Xth XXXXXXXXX 20XX, Accepted Xth XXXXXXXXX 20XX
DOI: 10.1039/b000000x

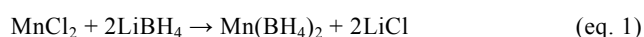
We have studied the reaction of MnCl₂ with MBH₄ (M = Li⁺, Na⁺, K⁺) in Et₂O. Crystal structures of two new intermediates, named [M(Et₂O)₂]₂Mn₂(BH₄)₅ (M = Li⁺, Na⁺), were elucidated by X-ray diffraction. Mn(BH₄)₂ in a mixture with LiBH₄ or NaBH₄ forms upon the solvent removal in vacuum.

¹⁰ [M(Et₂O)₂]₂Mn₂(BH₄)₅ contain 2D layers formed by Mn and BH₄ groups, linked through the alkali metal atoms coordinated to Et₂O. The loss of the solvent molecules leads to the segregation of the partially amorphous or nanocrystalline LiBH₄/NaBH₄ and a creation of the 3D framework of the crystalline Mn(BH₄)₂. While using LiBH₄ led to Mn(BH₄)₂ contaminated with LiCl, presumably due to an efficient trapping of the latter salt by the [Mn(BH₄)₂-Et₂O] system, the reaction with NaBH₄ produced chlorine-free Mn(BH₄)₂ accompanied with NaBH₄. Using KBH₄ led to the formation of K₂Mn(BH₄)₄ as a second phase. Two pyridine-containing solvomorphs, [Mn(py)₃(BH₄)₂] and [Mn(py)₄(BH₄)₂]·2py, were isolated in pure form. However, Mn(BH₄)₂ partly decomposes upon removal of pyridine molecules.

Introduction

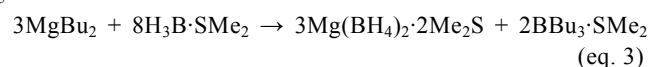
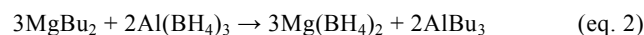
Borohydrides of alkali and alkali-earth metals are of interest ²⁰ as hydrogen storage materials, and they are even more intriguing as precursors to di-¹ or even trimetallic borohydrides² in order to tune the temperatures of dehydrogenation.^{3,4} Up to now, monometallic borohydrides have been obtained by both solvent based and ²⁵ mechanochemical syntheses,⁵ while mixed-metal borohydrides have usually been produced using mechanochemical syntheses.⁶ Very recently it was found that the latter borohydrides can also be obtained in solutions.⁷ Although borohydrides have been synthesized and ³⁰ characterized for many metals,^{3,7-11} the synthesis of manganese borohydride, Mn(BH₄)₂, obtained *via* ball-milling of MnCl₂ with LiBH₄ in a 1:2 ratio, has been reported only recently.¹² The crystal structure of Mn(BH₄)₂ was successfully determined from powder X-ray diffraction data. However, the ³⁵ suggested mechanochemical approach suffers from the presence of significant amounts of LiCl, limiting the use of the resulting product.

Another route to Mn(BH₄)₂ is the metathesis reaction between MnCl₂ and alkaline borohydrides in Et₂O.^{13,14} In ⁴⁰ particular, Schouwink *et al.* applied this method to obtain pure Mn(BH₄)₂ by reacting MnCl₂ and LiBH₄ in Et₂O (eq. 1).¹⁴



⁴⁵ However, this approach was not reproducible – only one synthesis was reported to be successful, whereas other

attempts failed due to the presence of LiCl in the final product. The same method was earlier applied by Černý *et al.* to obtain Mg(BH₄)₂, having a crystal structure similar to ⁵⁰ Mn(BH₄)₂.¹⁵ However, the resulting product was also contaminated by LiCl, Li₂MgCl₄ and LiBH₄. Pure Mg(BH₄)₂ was obtained using the reaction of Et₃NBH₃ and MgH₂.^{16,17} Because of the similarity between the structures, one may attempt to obtain pure Mn(BH₄)₂ by following the synthetic ⁵⁵ procedures to Mg(BH₄)₂. In particular, the latter borohydride can be obtained by reacting MgBu₂ either with Al(BH₄)₃ (eq. 2) or BH₃·Me₂S (eq. 3).^{18,19} Applying both synthetic procedures to Mn(BH₄)₂ requires manganese dialkyl precursors, which are either highly unstable at ambient ⁶⁰ conditions²⁰ and/or commercially unavailable. Furthermore, the use of Al(BH₄)₃ is not practical because of its high instability and explosiveness.



With all these in mind, we have drawn our attention to ⁷⁰ obtaining pure Mn(BH₄)₂ by synthesizing first its solvate, followed by removing solvent molecules from the structure. Unlike Mn(BH₄)₂, solvates of Mg(BH₄)₂ have extensively been studied.^{18,19,21-23} These results are of importance as a guideline to manganese-containing derivatives because of the ⁷⁵ structural and properties similarity of the corresponding analogues of Mn²⁺ and Mg²⁺ (salts, borohydrides, *etc.*).²⁴

Thus, we can suggest the same order of increasing donor strength of the solvent molecules for $\text{Mn}(\text{BH}_4)_2$ as it was found for $\text{Mg}(\text{BH}_4)_2$: $\text{Et}_2\text{O} < \text{THF} < \text{NH}_2t\text{Bu} \approx \text{piperidine} < \text{pyridine} < \text{benzylamine} < \text{DMSO}$.²¹ In order to facilitate solvent removal from the structure as well as to avoid a decomposition of the final $\text{Mn}(\text{BH}_4)_2$, the solvent molecules should be small and form weak interactions with the neighboring molecules in the structure. The last members of this series lack these properties and, hence, are not suitable for our strategy. The most suitable solvents seem to be Et_2O and THF.

Makhaev *et al.* reported the synthesis of $\text{Mn}(\text{BH}_4)_2 \cdot \text{THF}$, $\text{NaBH}_4 \cdot \text{Mn}(\text{BH}_4)_2 \cdot 3\text{THF}$ (solid), $\text{Mn}(\text{BH}_4)_2 \cdot 2\text{THF}$ (yellow oil) and $\text{Mn}(\text{BH}_4)_2 \cdot 3\text{THF}$ (solid).²⁵ The structure of the latter complex was established. However, it was found that $\text{Mn}(\text{BH}_4)_2 \cdot 3\text{THF}$ transforms to $\text{Mn}(\text{BH}_4)_2 \cdot 2\text{THF}$, then followed by a complete decomposition of manganese borohydride during heating.^{26,27} This makes the THF solvates non-suitable for our approach.

In this work we report the synthesis of $\text{Mn}(\text{BH}_4)_2$ in Et_2O using MnCl_2 and MBH_4 ($\text{M} = \text{Li}^+, \text{Na}^+, \text{K}^+$) to examine the influence of the nature of alkali metal onto the purity of the final product. We also made a detailed study of intermediate compounds formed during the reaction. Results on using an even smaller dimethyl sulfide, Me_2S , as a solvent in synthesis of $\text{Mn}(\text{BH}_4)_2$ will be reported elsewhere.²⁸ It should be noted, that the main difference in using Et_2O and Me_2S as a reaction medium is that the former solvent contains the “hard” oxygen donor atom, which is more suitable to efficiently solvate “hard” metal cations such as Li^+ , Na^+ and K^+ . The latter

solvent, containing the “soft” sulfur donor atom, would efficiently solvate “soft” d -metal cation, *viz.* Mn^{2+} . Herein we present our results using the first, Et_2O -based, synthetic approach. This in-depth study will open an avenue for the synthesis of $\text{Mn}(\text{BH}_4)_2$. Furthermore, for comparison with the light Et_2O we studied also the reaction between MnCl_2 with NaBH_4 in a highly donor solvent, pyridine. Despite it allows to isolate pure complexes of $\text{Mn}(\text{BH}_4)_2$, their desolvation leads to a partial decomposition of $\text{Mn}(\text{BH}_4)_2$.

Results and discussion

In agreement with Schouwink *et al.*,¹⁴ as well as it was also established for $\text{Mg}(\text{BH}_4)_2$,²⁹ our numerous experiments revealed that the metathesis reaction between MnCl_2 and LiBH_4 in Et_2O (eq. 1) was not reproducible to deliver pure $\text{Mn}(\text{BH}_4)_2$. Note, that this approach is based on the fact that both MnCl_2 and LiCl are poorly soluble in Et_2O , while $\text{Mn}(\text{BH}_4)_2$ efficiently soluble in this solvent.

Our results demonstrate the formation of $\text{Mn}(\text{BH}_4)_2$, containing about 35 wt. % of LiCl upon reacting MnCl_2 with LiBH_4 in Et_2O . We believe that, although LiCl is extremely poorly soluble in pure Et_2O (Table 1), it can be efficiently trapped by the $[\text{Mn}(\text{BH}_4)_2\text{-Et}_2\text{O}]$ system, for example *via* formation of more complex intermediates, thus increasing the solubility. Another reason might come from the formation of very small particles of LiCl during the reaction, which cannot be filtered out even using the PTFE membrane filter (22 μm pores).

Table 1 Solubility of the reported compounds at 25 °C^a

	LiCl	KCl	LiBH ₄	NaBH ₄	KBH ₄	MnCl ₂
Et ₂ O	0.77 mg/100 g, ³⁰ 0.6 mg/100 g ³¹	—	1.4 M, ³¹ 7.53 wt. %, ³² 4.5 wt. % ³³	insoluble, ^{31,34} 0.02 g/100 g ³⁵	insoluble ⁶	poorly soluble ³⁶
Dioxane	2.7 g/100 g ³¹	—	—	—	—	poorly soluble ³⁶
Pyridine	14.0 g/100 g, ³⁷ 10.0 g/100 g ³⁸	0.002 g/l ³⁸	—	3.4 g/100 g ³⁹	—	—
THF	4.3 g/100 g ⁴⁰	—	11.43 M, ³¹ 22.2 g/100 g ⁴¹	0.07 g/100 g, ³¹ 0.1 g/100 g, ³⁹ 0.04 wt. % ⁴²	insoluble ⁶	soluble ³⁶

^a No data were found for NaCl .

Thus, using LiBH_4 , as a borohydride source for the synthesis of $\text{Mn}(\text{BH}_4)_2$ in Et_2O , seems to be non-reliable due to the formation of LiCl , which significantly contaminates the resulting product. With this in mind, we have focused on alternative borohydride sources such as NaBH_4 and KBH_4 . Both precursors, as well as NaCl and KCl , are much less soluble in Et_2O compared to the corresponding lithium analogues (Table 1). Thus, using NaBH_4 and KBH_4 increased the reaction time significantly. It is worth to note, that before our investigations LiBH_4 , being the most reactive alkali-metal borohydride, was the only source of borohydride to produce $\text{Mn}(\text{BH}_4)_2$. Thus, our studies on using both NaBH_4 and KBH_4 to react with MnCl_2 in solutions were challenging. However, one would expect similar reaction properties of NaBH_4 and KBH_4 as for LiBH_4 to produce $\text{Mn}(\text{BH}_4)_2$.

Slow evaporation of the solvent from the reaction mixture of MnCl_2 with MBH_4 ($\text{M} = \text{Li}^+, \text{Na}^+, \text{K}^+$) in Et_2O led to yellow oil, which might be the result of the formation of mono- and/or polymetallic borohydrides with a high content of Et_2O . The solvent molecules might both coordinate to the metal centers and serve as lattice solvents trapped within voids upon crystallization. Makhaev *et al.* reported, that transition metal borohydrides form solvates with polyethers of the general formula $\text{NaM}^{n+}(\text{BH}_4)_{n+1} \cdot x\text{Solv}$ ($\text{M} = \text{V}, \text{Fe}, \text{Mn}$; $\text{Solv} = \text{dimethoxyethane}, \text{bis}(2\text{-methoxyethyl}) \text{ ether}, \text{THF}$).^{43,44}

All our attempts to crystallize the collected oils in a glass capillary by cooling down to 100 K have failed. Further slow drying of these oils under vacuum yielded yellow crystalline materials. Crystals obtained in NaBH_4 -based synthesis were suitable for single-crystal X-ray diffraction. According to

single-crystal and powder X-ray diffraction data, materials formed from the LiBH₄- and NaBH₄-based syntheses are corresponding dimetallic borohydride solvates [$\{M(\text{Et}_2\text{O})_2\}_2\text{Mn}_2(\text{BH}_4)_5$] (M = Li⁺, sample *Li_solv*; Na⁺, sample *Na_solv*). The bulk material of the *Li_solv* sample also contained LiCl. Further slow drying of these two samples led to the decomposition of dimetallic borohydrides with the formation of Mn(BH₄)₂ and the corresponding MBH₄ (M = Li⁺, sample *Li_dry*; Na⁺, sample *Na_dry*). However, only peaks for Mn(BH₄)₂ and LiCl, and Mn(BH₄)₂ and traces of NaBH₄ were found in the powder X-ray diffraction patterns of

Li_dry and *Na_dry*, respectively. This might be explained by the complete, for M = Li⁺, and partial for M = Na⁺, amorphization of the released MBH₄, as well as by very small size of the segregating MBH₄ particles. The KBH₄-based synthesis produced a mixture of Mn(BH₄)₂ and K₂Mn(BH₄)₄, with the latter compound being a minor product (~4 wt. %) (sample *K_dry*). K₂Mn(BH₄)₄ has been previously obtained from the mechanochemical synthesis.¹⁴ Thus, although 25% excess of MnCl₂ was used in the reactions with MBH₄ (M = Li⁺, Na⁺, K⁺), a strong affinity to form bimetallic structures was observed in all three cases.

Table 2 Unit cell parameters of the reported compounds

	[$\{\text{Li}(\text{Et}_2\text{O})_2\}_2\text{Mn}_2(\text{BH}_4)_5$]	[$\{\text{Na}(\text{Et}_2\text{O})_2\}_2\text{Mn}_2(\text{BH}_4)_5$]	[Mn(py) ₃ (BH ₄) ₂]	[Mn(py) ₄ (BH ₄) ₂]·2py	[Mg(py) ₄ (BH ₄) ₂]·2py ²²
Space group	<i>C2/c</i>	<i>C2</i>	<i>C2/c</i>	<i>Ccca</i>	<i>Ccca</i>
<i>Z</i>	4	2	4	4	4
<i>a</i> , Å	21.7106(3)	14.5133(6)	12.3618(4)	11.516(2)	11.604(2)
<i>b</i> , Å	7.72944(12)	7.4487(3)	15.5064(5)	14.938(4)	15.114(2)
<i>c</i> , Å	14.02422(19)	10.7119(5)	9.2859(4)	17.263(8)	17.190(2)
β , °	110.8649(14)	104.338(5)	101.126(4)	90	90
<i>V</i> , Å ³	2199.09(6)	1121.96(9)	1746.53(11)	2970(2)	3014.7(7)
CCDC	985621	985622	985623		186648

25

Cite this: DOI: 10.1039/coxx00000x

www.rsc.org/xxxxxx

ARTICLE TYPE

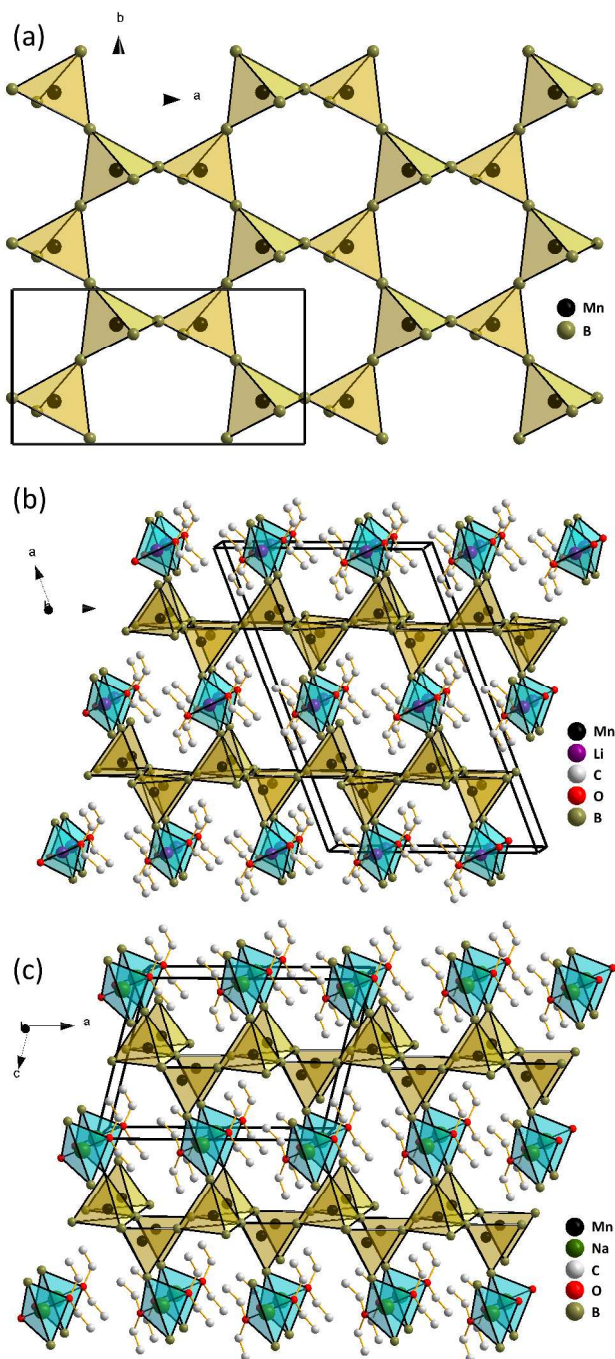


Fig. 1 The 2D layer formed by the MnB₄-based coordination tetrahedra in the structures of [M(Et₂O)₂]Mn₂(BH₄)₅ (M = Li⁺, Na⁺) (a). Crystal packing of [Li(Et₂O)₂]Mn₂(BH₄)₅ (b) and [Na(Et₂O)₂]Mn₂(BH₄)₅ (c). Polyhedra around the Mn atoms are shown in yellow, while those around the Li and Na atoms are given in blue. Hydrogen atoms were omitted.

According to X-ray diffraction data, [Li(Et₂O)₂]Mn₂(BH₄)₅ and [Na(Et₂O)₂]Mn₂(BH₄)₅

crystallize in the monoclinic space groups *C2/c* and *C2*, respectively (Table 2). The volume of the unit cell differs by roughly a factor of two, however the topology of the two structures is identical. Reconstruction of the reciprocal space sections for [Na(Et₂O)₂]Mn₂(BH₄)₅ did not show cell doubling in any direction, while the powder data for the Li-containing analogue clearly reveals superstructure peaks. The asymmetric unit in both compounds contains one Mn²⁺ cation, two BH₄⁻ anions in general positions and one on the 2 axis, one Et₂O molecule in a general position, and Li⁺ or Na⁺ cations in a special position. In both structures, each of the Mn²⁺ atoms coordinates four tetrahedral BH₄⁻ anions via edges with the formation of a slightly distorted Mn(BH₄)₄ tetrahedron. In the Li-containing compounds, the orientation of the BH₄⁻ groups cannot be reliably determined from the powder X-ray diffraction data. However, besides the orientation of the BH₄⁻ groups, other distances in the lithium structure can be determined quite precisely. The Mn–B bond distances are 2.280(7)–2.581(7) Å [2.329–2.497 Å; hereinafter the bond distances for the DFT-optimized structures are given in the brackets] and 2.403(11)–2.475(9) [2.383–2.452] Å in the Li- and Na-based structures, respectively. These values are comparable with those for pure Mn(BH₄)₂ and other compounds containing Mn²⁺ and BH₄⁻ fragments. Li⁺ or Na⁺ atoms are coordinated *via* edges to two BH₄⁻ groups with the Li–B and Na–B distances being 2.555(6) [2.582–2.566] and 2.700(11) [2.748] Å, respectively. Tetrahedral coordination spheres of Li⁺ and Na⁺ are further filled with two oxygen atoms from two Et₂O molecules with the Li–O and Na–O bond lengths 2.0030(14) [1.995–2.003] and 2.316(10) [2.377] Å, respectively. In both compounds, the BH₄⁻ group serves as a bridging ligand with respect to the two metal atoms, as in the solvent-free bimetallic borohydrides of transition metals (Zn²⁺, Mn²⁺, Sc³⁺, Cd²⁺, Y³⁺).^{1,14,46–50}

Since the positions of the hydrogen atoms are difficult to determine unambiguously from X-ray diffraction, we made DFT calculation on the experimental structures, clarifying the coordination modes of BH₄⁻ groups. Both compounds are insulators with a band gap of 2.1 and 1.9 eV for [Li(Et₂O)₂]Mn₂(BH₄)₅ and [Na(Et₂O)₂]Mn₂(BH₄)₅, respectively. Optimized structures clearly show bidentate coordination of all BH₄⁻ groups with respect to metal atoms in both compounds. The symmetry of the DFT-optimized structure of [Li(Et₂O)₂]Mn₂(BH₄)₅ is lower, space group is *Cc* instead of *C2/c*. This happens due to small displacements of atoms, which don't change significantly the entire structure. Rietveld refinement in the space group *Cc* gives a good fit, but involves nearly twice as many refined parameters. Therefore, for the experimental structure we finally decide to keep the space group *C2/c*.

The Mn-based tetrahedra form 2D layers in the *bc* and *ac* planes for [Li(Et₂O)₂]Mn₂(BH₄)₅ and [Na(Et₂O)₂]Mn₂(BH₄)₅, respectively (Fig. 1). These 2D

layers are linked through the Li- or Na-containing tetrahedra producing 3D structures (Fig. 1). Molecules of Et₂O are located between the 2D layers formed by Mn-based polyhedra (Fig. 1), which could explain the relatively easy release of the solvate molecules from the structures in vacuum. The 2D layers formed by Mn-based polyhedra are almost the same in both structures, but the layers of alkali metal based polyhedra are different. In the structure of [Na(Et₂O)₂]Mn₂(BH₄)₅, all Na-based polyhedra are oriented in the same way, while in the structure of [Li(Et₂O)₂]Mn₂(BH₄)₅, the Li-based polyhedra alternate with two different orientations, that results in the double cell for this compound, compared to the Na-containing analogue. But even taking into account this difference, the structures remain topologically similar. A 2D honeycomb topology of the Mn-based tetrahedra suggests that the magnetic ordering might be complex at low temperatures.⁵¹ But magnetic ordering cannot be directly detected by X-ray diffraction, and it is not present at the temperatures of interest – thus it is unrelated to the present study.

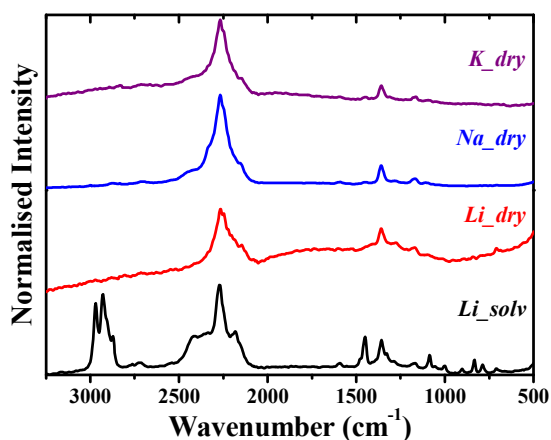


Fig. 2 Raman spectra of *Li_solv*, *Li_dry*, *Na_dry* and *K_dry*. The spectrum of *Na_solv* is similar to that of *Li_solv*.

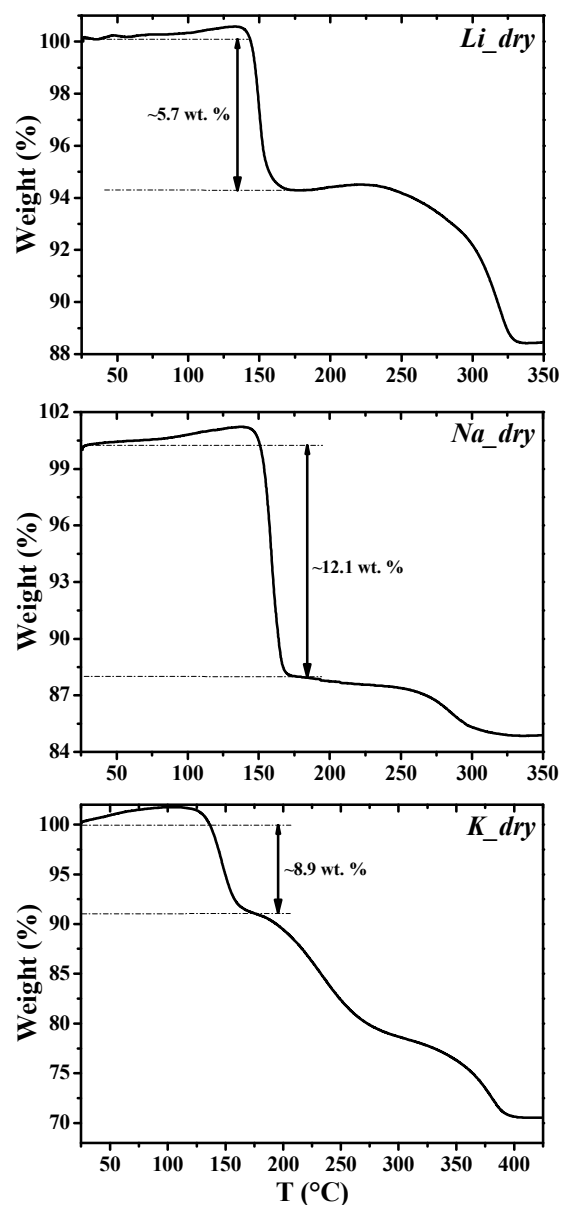
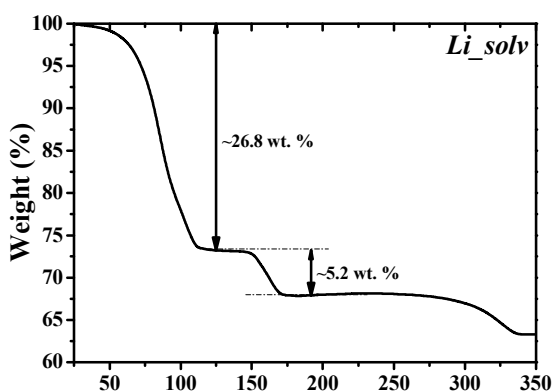


Fig. 3 TG analyses of *Li_solv*, *Li_dry*, *Na_dry* and *K_dry* performed in a dynamic argon atmosphere. The TG data for *Na_solv* are similar to those of *Li_solv*. All mass loss steps were found to be endothermic.

We suggest that evaporation of the molecules of Et₂O breaks the coordination environment around the Li⁺ or Na⁺ atoms, leading to a collapse of the structure with the formation of Mn(BH₄)₂ and corresponding MBH₄ (M = Li⁺, Na⁺).

The Raman spectra of *Li_solv*, *Li_dry*, *Na_dry* and *K_dry* (Fig. 2) contain characteristic bands for the BH₄⁻ groups, seen also in the structure of Mn(BH₄)₂.¹⁶ Furthermore, the Raman spectrum of *Li_solv* exhibits a set of characteristic bands for the Et₂O molecules: medium bands at 1360 and 1450 cm⁻¹ as well as number of intense bands at 2820–3020 cm⁻¹, corresponding to the CH vibrations of the ethyl groups; and a weak band at about 1090 cm⁻¹, which is typical for the COC asymmetric stretches. It should be noted, that no bands for the

Et₂O molecules were found in the Raman spectra of *Li_dry*, *Na_dry* and *K_dry* testifying the complete evaporation of the solvent molecules.

The thermal properties of *Li_solv*, *Li_dry*, *Na_dry* and *K_dry* in an argon atmosphere were studied by means of the TG analysis (Fig. 3). *Li_solv* is stable up to about 35 °C and decomposed in three clearly (despite the mass drift) defined steps. The first remarkable step up to about 110 °C corresponds to the evolution of Et₂O. The second mass loss up to about 160 °C is due to the decomposition of Mn(BH₄)₂.^{28,52} It should be noted that this decomposition step was found in the TG data of all compounds (Fig. 3). However, the temperature-dependent *in situ* powder X-ray diffraction data, collected for *Li_solv*, exhibit peaks exclusively for LiCl after about 105 °C accompanied with new very broad humps due to the formation of the either amorphous or liquid phase, containing dissolved Mn(BH₄)₂ and LiBH₄ (Fig. 4). The observed discrepancies between the TG and powder X-ray diffraction data might be explained by different experimental conditions. In particular, the latter experiments were done in the capillary sealed by wax, which can be considered as a “closed” system, while TG studies were performed in a crucible under a flow of argon, thus, in an “open” system. The latter system favors an efficient removal of the evaporated Et₂O, while it is blocked in the former system. This, in turn, leads to dissolving of the crystalline borohydride residues, released during the decomposition (Table 1). However, LiCl remains intact upon applied experimental conditions due to its, first, poor solubility in Et₂O (Table 1) and, second, high thermal stability.

The TG for *Li_dry* is very similar to that of *Li_solv* after the latter compound completely loses Et₂O (Fig. 3). The TG data for *Na_dry* and *K_dry*, with the first step of mass loss due to the decomposition of Mn(BH₄)₂, show the same features as *Li_dry* (Fig. 3). However, since the sample *K_dry* contains also K₂Mn(BH₄)₂, its TG is, obviously, complicated by the decomposition pathway of this bimetallic borohydride.¹⁴

Various solvates of the same borohydride could be used to produce new polymorphs. In particular, porous polymorphs, which are even more promising for gas storage. For example, porous γ -Mg(BH₄)₂ was successfully obtained from the Mg(BH₄)₂·0.5Me₂S solvate.¹⁹ However, the formation of a stable borohydride from its solvate requires that the parent structure comprises a rigid 3D framework formed by coordination polyhedra around the metal atoms, or at least the presence of rigid 3D fragments. As we described above, both dimetallic solvates exhibit exclusively 2D Mn-BH₄ layers. The loss of the solvent molecules leads to the segregation of the partially amorphous or nanocrystalline LiBH₄/NaBH₄ and a creation of the new 3D framework of the crystalline Mn(BH₄)₂. The behaviour of the mononuclear pyridine complexes of Mn(BH₄)₂, obtained in this work, illustrates that the formation of stable borohydrides from their solvates is difficult in the absence of rigid metal-borohydride frameworks present already in the parent structure.

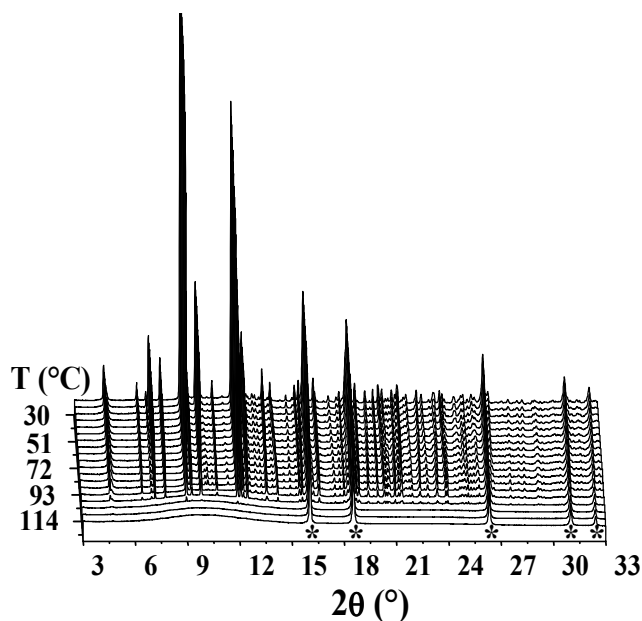


Fig. 4 *In-situ* synchrotron X-ray diffraction on *Li_solv* measured from 30 to 130 °C ($\lambda = 0.82742$ Å). $[\{\text{Li}(\text{Et}_2\text{O})_2\}\text{Mn}_2(\text{BH}_4)_3]$ decomposes at about 105 °C. Peaks from the LiCl phase are marked with asterisks.

The reaction of MnCl₂ with NaBH₄ in pyridine produces at least two solvates, $[\text{Mn}(\text{py})_3(\text{BH}_4)_2]$ and $[\text{Mn}(\text{py})_4(\text{BH}_4)_2] \cdot 2\text{py}$. According to single-crystal X-ray diffraction data the former complex crystallizes in the monoclinic *C2/c* space group and exhibits a heteroleptic mononuclear complex (Figure 5, Table 2). The asymmetric unit contains one BH₄⁻ anion, one molecule of pyridine in general and one in special positions, and one Mn²⁺ cation on the 2-fold axis, which results in a molecular complex with the C₂ symmetry. The Mn²⁺ atom coordinates two tetrahedral BH₄⁻ anions *via* the edges at Mn–B distances of 2.483(2) Å. The coordination sphere of the metal center is completed by three nitrogen atoms from three pyridine molecules. The Mn–N bond distances are 2.246(3) and 2.2823(19) Å. The coordination environment of Mn can be described either as square-pyramidal or trigonal bipyramidal depending on the parameter $\tau = (\beta - \alpha)/60$, where α and β are the two largest bond angles around the metal ion. An ideal square pyramidal arrangement is described by the value of $\tau = 0$, while an ideal trigonal bipyramidal arrangement has the value of $\tau = 1$.⁵² The largest bond angles in the coordination sphere of Mn²⁺ are 175.92(8) and 127.72(11)°. This gives τ value of 0.8, which is significantly closer to that of the ideal trigonal bipyramidal around the metal atom. The equatorial plane of the bipyramid is formed by both BH₄⁻ anions and one of the pyridine molecules.

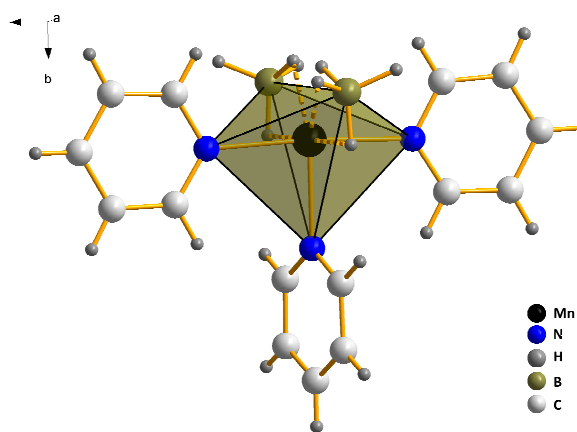


Fig. 5 Molecular structure of $[\text{Mn}(\text{py})_3(\text{BH}_4)_2]$.

Unfortunately, we were not able to obtain single crystals of $[\text{Mn}(\text{py})_4(\text{BH}_4)_2] \cdot 2\text{py}$ suitable for structure determination. However, we were successful to determine the space group and the unit cell parameters. Based on the obtained data, we suggest that $[\text{Mn}(\text{py})_4(\text{BH}_4)_2] \cdot 2\text{py}$ is isostructural to the previously reported complex $[\text{Mg}(\text{py})_4(\text{BH}_4)_2] \cdot 2\text{py}$.²¹ (Table 2). Thus, the manganese derivative comprises a discrete heteroleptic mononuclear complex $[\text{Mn}(\text{py})_4(\text{BH}_4)_2]$ and two lattice pyridine molecules (Figure 6). The Mn^{2+} cation coordinates four pyridine molecules and two BH_4^- anions forming a distorted octahedron.

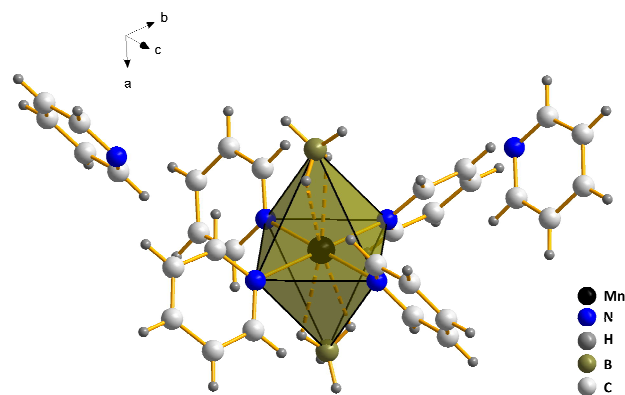


Fig. 6 Molecular structure of $[\text{Mn}(\text{py})_4(\text{BH}_4)_2] \cdot 2\text{py}$.

Both pyridine-containing solvomorphs contain mononuclear Mn complexes, which are well isolated from each other. The departure of the solvent molecules leads to a complete structural rearrangement accompanied by $\text{Mn}(\text{BH}_4)_2$ decomposition and gas release. The structures contain no polymeric chains to form relatively stable frameworks, and they turn out to be not suitable as precursors for obtaining neither porous nor even dense $\text{Mn}(\text{BH}_4)_2$ polymorphs. However, both pyridine complexes described in this work, as well as the previously reported magnesium analogue,²² are an intriguing starting point for the possible formation of porous metal organic borohydride frameworks using polypyridine

ligands as organic linkers aiming for different topologies and porosity, like for example described in the work of Ingleson *et al.*⁵⁴

Conclusions

In summary, we have studied the synthetic pathway to $\text{Mn}(\text{BH}_4)_2$ by reacting MnCl_2 and alkali metal borohydrides in diethyl ether. The two new solid intermediates $[\{\text{M}(\text{Et}_2\text{O})_2\}\text{Mn}_2(\text{BH}_4)_5]$ ($\text{M} = \text{Li}^+, \text{Na}^+$) were isolated and characterized. We found that pure $\text{Mn}(\text{BH}_4)_2$ could not be obtained by this approach because of the inclusion of LiBH_4 or NaBH_4 leading to the stable bimetallic solvates that were isolated from the reaction mixture. Moreover, using of LiBH_4 is less favorable due to the efficient trapping of LiCl by the $[\text{Mn}(\text{BH}_4)_2-\text{Et}_2\text{O}]$ system. Using NaBH_4 allows to obtain $\text{Mn}(\text{BH}_4)_2$ with some of the starting borohydride, while KBH_4 leads to $\text{Mn}(\text{BH}_4)_2$ contaminated by $\text{K}_2\text{Mn}(\text{BH}_4)_4$.

We have also obtained two new pyridine solvates of $\text{Mn}(\text{BH}_4)_2$, by reacting MnCl_2 with NaBH_4 in pyridine. Both solvomorphs consist of mononuclear complexes of Mn, that are not suitable as precursors for pure $\text{Mn}(\text{BH}_4)_2$, as it partly decomposes upon removal of pyridine molecules.

Experimental

Materials

All experiments were performed under anhydrous conditions by use of Schlenk techniques and argon as a protecting gas. All materials were used as received and without further purification: MnCl_2 (Sigma-Aldrich, anhydrous, 99.99%), LiBH_4 (Sigma-Aldrich, $\geq 95\%$), NaBH_4 (Alfa Aesar, $\geq 97\%$), (Sigma-Aldrich, $\geq 99.9\%$), Et_2O (VWR, $\text{H}_2\text{O} < 11$ ppm), pyridine (Sigma-Aldrich, anhydrous, 99.8%).

Analytical methods

Raman spectra were obtained with a FTIR Nicolet Magna 860 with Raman unit and Nd:YVO₄ ($\lambda = 1064$ nm) laser. Samples were placed in glass capillaries in inert atmosphere and sealed with vacuum grease. Thermogravimetric analysis was done using a SDT 2960 Simultaneous DTA-TGA instrument in a dynamic argon atmosphere (100 mL min^{-1}) from ambient temperature to 600°C with a 5°C/min heating rate.

Synthesis

Reaction of MnCl_2 with LiBH_4 in Et_2O . A pink suspension of MnCl_2 (2.52 g, 20.0 mmol) and LiBH_4 (0.70 g, 32.0 mmol) in Et_2O (120 mL) was vigorously stirred for about 24 h. The resulting mixture was filtered using first a microporous glass filter and then the PTFE membrane filter ($22 \mu\text{m}$ pores). The filtrate was slowly (~ 2 h) concentrated in vacuum at room temperature. During concentration, a fine crystalline white powder of LiCl was precipitated alongside with the formation of pale yellow oil. Further concentration yielded a pale yellow solid material (sample *Li_solv*, sample designations and phase content are summarized in Table 3), which was characterized, according to the powder X-ray diffraction data, as a mixture

of [$\text{Li}(\text{Et}_2\text{O})_2\text{Mn}_2(\text{BH}_4)_5$] (79.4 wt. %) and LiCl (20.6 wt. %). The solid material was further dried in vacuum at room temperature for about 2.5 days. The resulting pale yellow powder (sample *Li_dry* in Table 3) was characterized, according to the powder X-ray diffraction data, as a mixture of $\text{Mn}(\text{BH}_4)_2$ (65 wt. %) and LiCl (35 wt. %). Based on the composition of the initial sample, the final product should contain $\text{Mn}(\text{BH}_4)_2$ (61.5 wt. %) LiCl (30.7 wt. %) and LiBH_4 (7.9 wt. %). However, the powder X-ray diffraction pattern did not exhibit peaks for LiBH_4 , which is, probably, due to the amorphization of the latter compound or very small size of its particles.

Reaction of MnCl_2 with NaBH_4 in Et_2O . A pink suspension of MnCl_2 (2.52 g, 20.0 mmol) and NaBH_4 (1.21 g, 32.0 mmol) in Et_2O (120 mL) was vigorously stirred for several days until a clear yellow solution with white precipitate appeared. The reaction proceeded much slower than the analogous reaction with LiBH_4 due to a lower solubility of NaBH_4 in Et_2O . The resulting mixture was filtered using a microporous glass filter. The filtrate was slowly concentrated and the formation of pale yellow oil was observed. Further slow drying of this oil in vacuum at room temperature resulted in yellow crystals (sample *Na_solv* in Table 3), according to the single-crystal and powder X-ray diffraction data, of [$\text{Na}(\text{Et}_2\text{O})_2\text{Mn}_2(\text{BH}_4)_5$]. The solid material was further dried in vacuum at room temperature for about 2.5 days. The resulting pale yellow powder (sample *Na_dry* in Table 3) was characterized, according to the powder X-ray diffraction data, as a mixture of $\text{Mn}(\text{BH}_4)_2$ (94 wt. %) and NaBH_4 (6 wt. %). Based on the composition of the initial sample, the final product should contain about 30.9 wt. % of NaBH_4 . The

Table 3 Phase composition of samples

Sample name	Phases	wt. %, experimental X-ray data	wt. %, calculated from the initial composition
<i>Li_solv</i>	[$\text{Li}(\text{Et}_2\text{O})_2\text{Mn}_2(\text{BH}_4)_5$]	79.4	—
	LiCl	20.6	
<i>Li_dry</i>	$\text{Mn}(\text{BH}_4)_2$	65	61.5
	LiBH_4	0	7.9
	LiCl	35	30.7
<i>Na_solv</i>	[$\text{Na}(\text{Et}_2\text{O})_2\text{Mn}_2(\text{BH}_4)_5$]	100	—
<i>Na_dry</i>	$\text{Mn}(\text{BH}_4)_2$	94	69.1
	NaBH_4	6	30.9
<i>K_dry</i>	$\text{Mn}(\text{BH}_4)_2$	96	—
	$\text{K}_2\text{Mn}(\text{BH}_4)_4$	4	

Single crystal X-ray crystallography

The X-ray data were collected at 150(2) K on a MAR345 image plate detector using Mo $K\alpha$ radiation (Rigaku UltraX 18 rotation anode, Xenocs Fox3D focusing multilayer mirror). The data were integrated with the CrysAlisPro software.⁵⁵ The implemented multi-scan absorption correction was applied. The structures were solved by direct methods using the SHELXS-97⁵⁶ program and refined by full-matrix least squares on $|F|^2$ using SHELXL-97.⁵⁶ Non-hydrogen atoms were refined anisotropically, while hydrogen atoms of Et_2O

observed discrepancy is, most likely, due to a partial amorphization of NaBH_4 or very small size of its particles.

Reaction of MnCl_2 with KBH_4 in Et_2O . A pink suspension of MnCl_2 (2.52 g, 20.0 mmol) and KBH_4 (1.73 g, 32.0 mmol) in Et_2O (120 mL) was vigorously stirred for several days until a clear yellow solution with white precipitate appeared. The reaction proceeded much slower than the analogous reaction with LiBH_4 due to a lower solubility of KBH_4 in Et_2O . The resulting mixture was filtered using a microporous glass filter. The filtrate was slowly concentrated and the formation of pale yellow oil was observed. Further slow drying of this oil in vacuum at room temperature resulted to pale yellow solid, which was further dried in vacuum at room temperature for about 2.5 days. The resulting pale yellow powder (sample *K_dry* in Table 3) was characterized, according to the powder X-ray diffraction data, as a mixture of $\text{Mn}(\text{BH}_4)_2$ (96 wt. %) and $\text{K}_2\text{Mn}(\text{BH}_4)_4$ (4 wt. %).

Reaction of MnCl_2 with NaBH_4 in pyridine. A dark brown suspension of MnCl_2 (2.52 g, 20.0 mmol) and NaBH_4 (1.21 g, 32.0 mmol) in pyridine (py, 120 mL) was vigorously stirred for two days. The resulting mixture was filtered using the PTFE membrane filter (22 μm pores). The filtrate was slowly concentrated in vacuum at room temperature until colorless crystals were formed. These crystals were stable in the mother liquor at room temperature for few hours, but quickly decomposed at room temperature when isolated from the solution, even under inert conditions. At least two pyridine-containing compounds, $[\text{Mn}(\text{py})_3(\text{BH}_4)_2]$ and $[\text{Mn}(\text{py})_4(\text{BH}_4)_2]\cdot 2\text{py}$, were obtained, according to the single-crystal X-ray diffraction data.

were localized from a differential Fourier map, but were placed on calculated positions in a riding mode with temperature factors fixed at 1.2 times U_{eq} of the parent atoms and 1.5 times U_{eq} for the methyl groups. The B–H and H–H distances in the BH_4 groups were constrained to form ideal tetrahedrons. Inspection of the differential Fourier map revealed a presence of positional disorder in Et_2O . Attempts to model this disorder with several fixed positions of the Et_2O molecule resulted to an insignificant improvement of the model, so we modeled the disorder with higher temperature factors of the atoms.

Synchrotron powder X-ray crystallography

The synchrotron radiation powder X-ray diffraction data were collected at the Swiss-Norwegian beamline BM1A at the European Synchrotron Radiation Facility (ESRF) (Grenoble, France) using a PILATUS 2M pixel detector. The wavelength was 0.82742 Å, and the sample-to-detector distance was 430 mm. These parameters along with image plate tilt angles were calibrated using a standard LaB₆ sample. The *Li_solv* sample was sealed in the thin-walled glass capillary under argon atmosphere and measured at 100(2) K. Two-dimensional diffraction images from this sample were integrated using the ESRF Fit2D program.⁵⁷ The pattern was indexed using DICVOL04⁵⁸ in a centered monoclinic crystal system. Analysis of systematic absences suggested the *C2/c* and *Cc* space groups. Based on the assumed composition, Mn(BH₄)₂·x(C₂H₅)₂O, and an approximate volume of the Mn(BH₄)₂ unit being 113 Å³, and the volume of the Et₂O molecule being 125 Å³, we suggested the composition of 3Mn(BH₄)₂·2Et₂O. However, attempts to solve the structure applying this composition by global optimization in direct space in the FOX⁵⁹ program failed. The occupancy of all but one Mn atoms was close to 0. Therefore, we suggested the presence of Li atoms along with Mn in the structure. The structure was finally solved and refined in the *C2/c* space group with a composition of [*Li*(Et₂O)₂]*Mn*₂(BH₄)₅. In the final refinement, antibump restraints were 3 Å for the O–O and B–O contacts, 1.8 Å for O–H, 2.8 Å for B–C and Mn–C, 2.2 Å for H–H, and of 3.3 Å for B–B distances. The final refinement was done with the *C2/c* space group using the Rietveld method in the Fullprof suite software.⁶⁰ Coordinates of the Et₂O molecule were refined, with its orientation and configuration being fixed. The bond lengths in the Et₂O and BH₄ groups were constrained to be close to the following values: *d*(C–C) 1.50 Å, *d*(C–O) 1.425 Å, *d*(C–H)_{CH3} 0.97 Å, *d*(C–H)_{CH2} 0.96 Å, *d*(B–H) 1.13 Å, *d*(H–H)_{BH4} 1.841 Å. The bond angles were constrained using soft distance and angle constraints. The torsion angles of the CH₃ groups in Et₂O were constrained using distance constraints to prevent an eclipsed conformation. One of the BH₄ groups was found on the inversion center, and this group was disordered over two 50/50% orientations since the symmetry of the BH₄ group is incompatible with an inversion center. The orientation of this group was constrained using distance restraints to make all Mn–H distances equal. Overall, 52 distance constraints and 25 angle constraints were applied. The second phase, LiCl, was modeled, with a final weight fraction of 20.54(10)%. The background was described by a linear interpolation of the selected points. The final discrepancy factors were: *R*_B = 5.05%, *R*_F = 6.30%, *R*_p = 10.52% and *R*_{wp} = 11.29%. The refinement profile is shown in Fig. 5.

Laboratory powder X-ray crystallography

Powder X-ray diffraction data were collected on a MAR345 image plate detector using Mo K α radiation (Rigaku UltraX 18 rotation anode, Xenocs Fox3D focusing multilayer mirror). The two-dimensional diffraction images were integrated using the ESRF Fit2D⁵⁶ program. The integrated patterns were

treated using the Fullprof suite software.⁶⁰

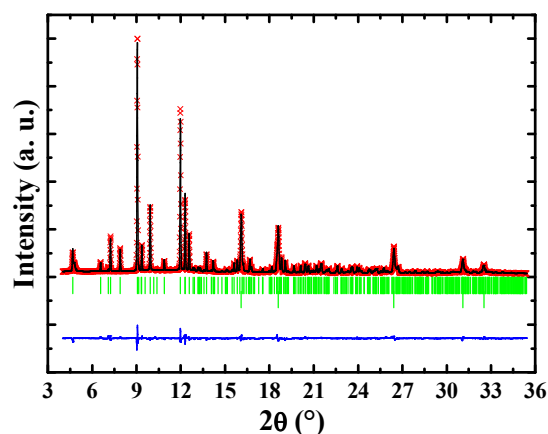


Fig. 5 Rietveld refinement plot for [*Li*(Et₂O)₂]*Mn*₂(BH₄)₅. Red crosses and black line show the experimental and calculated data, respectively. Blue line is the difference profile, and green marks indicate Bragg positions.

DFT calculations

The structures were optimized by conjugated gradient method within plane wave formulation of spin polarized density functional theory (DFT).⁶¹ Electronic configuration of 1s²2s¹ for Li, 2p⁶3s¹ for Na, 3d⁶4s¹ for Mn, 2s²2p² for C, 2s²2p⁴ for O, 2s²2p¹ for B, and 1s¹ for H was represented by projected augmented wave potentials.⁶² The gradient corrected (GGA) functional⁶³ was applied. The initial structure from the Rietveld refinement was optimized with respect to the internal atomic positions, the unit cell shape and volume was fixed. The on-site Coulomb repulsion⁶⁴ *U* = 4 was applied for the manganese *d* electrons. Since the manganese atoms are arranged on the honeycomb-like 2D networks (Fig. 1) the ground state magnetic ordering could be nontrivial. This is despite the fact of obvious antiferromagnetic superexchange interaction between each adjacent Mn²⁺ linked by the BH₄⁻ anion. For example the lowest energy state with collinear antiferromagnetic arrangement of sub-layers with up and down oriented BH₄⁻ tetrahedra is only 110 and 118 meV/formula unit more stable than the ferromagnetic one for [*Li*(Et₂O)₂]*Mn*₂(BH₄)₅ and [*Na*(Et₂O)₂]*Mn*₂(BH₄)₅, respectively. Moreover, it does not affect the structural configuration of the light atoms in the lattice. Noncollinear ordering of the magnetic moments requires larger superstructures, but around the room temperature they will not be present. We have checked that the total ground state energy for noncollinear spin arrangement varies on the scale of single or tenth of meV. Interestingly, in both compounds Mn formally is in the oxidation state 2+, however it is tetrahedrally coordinated by four BH₄⁻ anions. This coordination environment enforces a high spin arrangement of the Mn *d*-electrons. The calculated magnetic moments of Mn are 4.33 μ_B for the ferromagnetic, and ±4.29 or ±4.28 μ_B for the antiferromagnetic orders in [*Li*(Et₂O)₂]*Mn*₂(BH₄)₅ and [*Na*(Et₂O)₂]*Mn*₂(BH₄)₅, respectively. In order to avoid

complications related to the fact that numerical values of the magnetic moments depend on particular choice of the Hubbard U ,⁶⁵ possibility of induction of the dipole moments/ferroelectricity due to noncentrosymmetry, noncollinear spin arrangements on the honeycomb lattices⁵¹ overall resulting in the exotic magnetic configurations the antiferromagnetic ordering of Mn magnetic moments as described above was assumed. The crystal structures are almost the same regardless of the ferro and antiferro spin ordering. Each system was relaxed until forces exerted on atoms were below 0.01 eV/Å. For $[\text{Li}(\text{Et}_2\text{O})_2\text{Mn}_2(\text{BH}_4)_5]$ with a static disorder of BH_4^- groups two different ordered configurations of BH_4^- were assumed. Above mentioned assumptions are sources of errors, however we do not expect them to be larger than ~ 0.1 eV/formula unit, and they are of minor importance for the crystal structure.

CCDC 985621 ($[\text{Li}(\text{Et}_2\text{O})_2\text{Mn}_2(\text{BH}_4)_5]$), 985622 ($[\text{Na}(\text{Et}_2\text{O})_2\text{Mn}_2(\text{BH}_4)_5]$) and 985623 ($[\text{Mn}(\text{py})_3(\text{BH}_4)_2]$) contain the supplementary crystallographic data. These data can be obtained free of charge via <http://www.ccdc.cam.ac.uk/conts/retrieving.html>, or from the Cambridge Crystallographic Data Centre, 12 Union Road, Cambridge CB2 1EZ, UK; fax: (+44) 1223-336-033; or e-mail: deposit@ccdc.cam.ac.uk. DFT optimized structures of $[\text{Li}(\text{Et}_2\text{O})_2\text{Mn}_2(\text{BH}_4)_5]$ and $[\text{Na}(\text{Et}_2\text{O})_2\text{Mn}_2(\text{BH}_4)_5]$ are available as supplementary information.

Acknowledgements

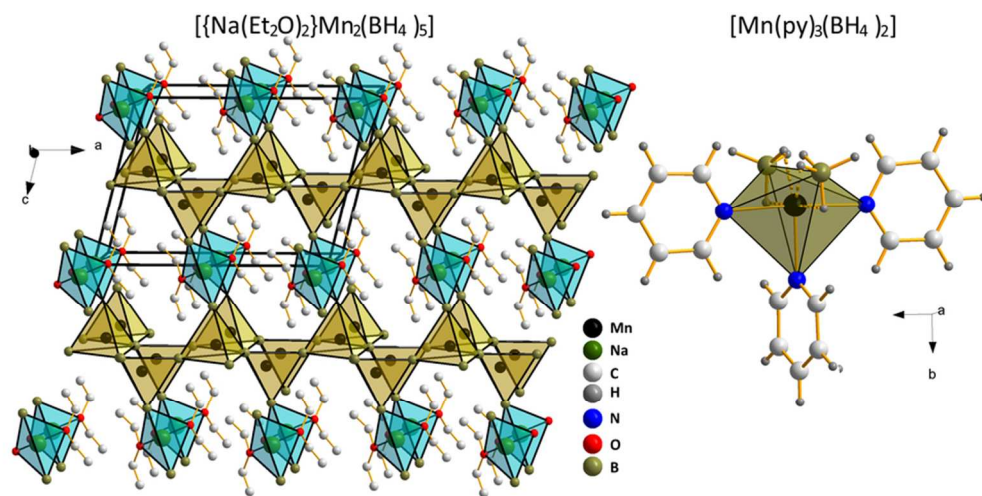
The authors FNRS (CC 1.5169.12, PDR T.0169.13, EQP U.N038.13) for financial support. We acknowledge the Fonds Spéciaux de Recherche (UCL) for the incoming postdoctoral fellowship co-funded by the Marie Curie actions of the European Commission granted to N. A. Tumanov and WBI (Belgium) for the postdoctoral position allocated to D. A. Safin. We thank ESRF for the beamtime allocation at the SNBL and V. Dyadkin for help, and A. Railliet for the help with thermogravimetric measurements. Part of this work was supported by the COST Action MP1103 "Nanostructured materials for solid-state hydrogen storage", by the Danish Council for Strategic Research, via the research project HyFillFast, the Danish National Research Foundation, Center for Materials Crystallography (DNRF93), and by the Danish Research Council for Nature and Universe (Danscatt). We acknowledge funding from the European Community's Seventh Framework Programme, the Fuel Cells and Hydrogen Joint Undertaking (FCH JU), project BOR4STORE (303428). We are grateful to the Carlsberg Foundation for support. Z. Łodziana acknowledges CPU allocation at the PLGrid Infrastructure and support by a grant from Switzerland through the Swiss Contribution to the enlarged European Union.

Notes and references

^a Institute of Condensed Matter and Nanosciences, Molecules, Solids & Reactivity (IMCN/MOST), Université Catholique de Louvain, Place L. Pasteur 1, 1348 Louvain-la-Neuve, Belgium. E-mail: yaroslav.filinchuk@uclouvain.be

- ^b Center for Materials Crystallography (CMC), Interdisciplinary Nanoscience Center (iNANO), and Department of Chemistry, Aarhus University, Langelandsgade 140, DK-8000 Århus C, Denmark.
- ^c INP Polish Academy of Sciences, Department of Structural Research, ul. Radzikowskiego 152, 31-342 Kraków, Poland.
- For crystallographic data in CIF or other electronic format see DOI: 10.1039/b000000x
- D. Ravnsbaek, Y. Filinchuk, Y. Cerenius, H. J. Jakobsen, F. Besenbacher, J. Skibsted and T. R. Jensen, *Angew. Chem. Int. Ed.*, 2009, **48**, 6659.
 - R. Černý, P. Schouwink, Y. Sadikin, K. Stare, L. Smrčok, B. Richter, and T. R. Jensen, *Inorg. Chem.*, 2013, **52**, 9941.
 - L. H. Rude, T. K. Nielsen, D. B. Ravnsbaek, U. Bösenberg, M. B. Ley, B. Richter, L. M. Arnbjerg, M. Dornheim, Y. Filinchuk, F. Besenbacher and T. R. Jensen, *Phys. Status Sol. A*, 2011, **208**, 1754.
 - Y. Nakamori, K. Miwa, A. Ninomiya, H. Li, N. Ohba, S. Towata, A. Züttel and S. Orimo, *Phys. Rev. B*, 2006, **74**, 045126.
 - H. Hagemann and R. Černý, *Dalton Trans.*, 2010, **39**, 6006.
 - J. Huot, D. B. Ravnsbaek, J. Zhang, F. Cuevas, M. Lacroche and T. R. Jensen, *Prog. Mater. Sci.*, 2013, **58**, 30.
 - T. Jaroń, P. A. Orłowski, W. Wegner, K. J. Fijałkowski, P. J. Leszczyński, and W. Grochala, *Angew. Chem. Int. Ed.*, 2015, **54**, 1236.
 - Y. Filinchuk, D. Chernyshov and V. Dmitriev, *Z. Kristallogr.*, 2008, **223**, 649.
 - M. B. Ley, L. H. Jepsen, Y.-S. Lee, Y. W. Cho, J. M. Bellosta von Colbe, M. Dornheim, M. Rokni, J. O. Jensen, M. Sloth, Y. Filinchuk, J. E. Jørgensen, F. Besenbacher and T. R. Jensen, *Mater. Today*, 2014, **17**, 122.
 - F. Pendolino, *J. Phys. Chem. C*, 2012, **116**, 1390.
 - L. H. Jepsen, M. B. Ley, Y.-S. Lee, Y. W. Cho, M. Dornheim, J. O. Jensen, Y. Filinchuk, J. E. Jørgensen, F. Besenbacher and T. R. Jensen, *Mater. Today*, 2014, **17**, 129.
 - R. Černý, N. Penin, H. Hagemann and Y. Filinchuk, *J. Phys. Chem. C*, 2009, **113**, 9003.
 - G. Monnier, *Ann. Chim. (Cachan, Fr.)*, 1957, **13**, 14.
 - P. Schouwink, V. D'Anna, M. B. Ley, L. M. Lawson Daku, B. Richter, T. R. Jensen, H. Hagemann and R. Černý, *J. Phys. Chem. C*, 2012, **116**, 10829.
 - R. Černý, Y. Filinchuk, H. Hagemann and K. Yvon, *Angew. Chem. Int. Ed.*, 2007, **46**, 5765.
 - Y. Filinchuk, R. Černý and H. Hagemann, *Chem. Mater.*, 2009, **21**, 925.
 - K. Chłopek, C. Frommen, A. Léon, O. Zabara and M. Fichtner, *J. Mater. Chem.*, 2007, **17**, 3496.
 - P. Zanella, L. Crociani, N. Masciocchi and G. Giunchi, *Inorg. Chem.*, 2007, **46**, 9039.
 - Y. Filinchuk, B. Richter, T. R. Jensen, V. Dmitriev, D. Chernyshov and H. Hagemann, *Angew. Chem. Int. Ed.*, 2011, **50**, 11162.
 - M. Tamura and J. Kochi, *J. Organomet. Chem.*, 1971, **29**, 111.
 - M. Bremer, G. Linti, H. Nöth, M. Thomann-Albach and G. E. W. J. Wagner, *Z. Anorg. Allg. Chem.*, 2005, **631**, 683.
 - M. Bremer, H. Nöth and M. Warchhold, *Eur. J. Inorg. Chem.*, 2003, 111.
 - G. L. Soloveichik, M. Andrus and E. B. Lobkovsky, *Inorg. Chem.*, 2007, **46**, 3790.
 - R. Černý, N. Penin, V. D'Anna, H. Hagemann, E. Durand and J. Růžička, *Acta Mater.*, 2011, **59**, 5171.
 - V. D. Makhaev, A. P. Borisov, T. P. Gnilomedova, E. B. Lobkovskii and A. N. Chekhlov, *Bull. Acad. Sci. USSR Div. Chem. Sci.*, 1987, **36**, 1582.
 - V. D. Makhaev, A. P. Borisov, T. P. Karpova and L. A. Petrova, *Russ. J. Inorg. Chem.*, 1995, **40**, 1579.
 - V. D. Makhaev, *Priv. Commun.*, 2014.
 - B. Richter, N. A. Tumanov, D. B. Ravnsbaek, Y. Filinchuk and T. R. Jensen, *Dalton Trans.*, 2015, DOI: 10.1039/C4DT03501A.
 - G. L. Soloveichik, M. Andrus, Y. Gao, J.-C. Zhao and S. Kniažanski, *Int. J. Hydrogen Energy*, 2009, **34**, 2144.
 - S. K. Sharov, L. P. Portnov, L. P. Ivanov and A. I. Gorbunov, *Russ. J. Phys. Chem.*, 1987, **61**, 1405.

- 31 H. C. Brown, Y. M. Choi and S. Narasimhan, *Inorg. Chem.*, 1982, **21**, 3657.
- 32 D. A. Brandreth and M. C. Molstad, *J. Chem. Eng. Data*, 1962, **7**, 449.
- 5 33 V. Mikheeva and E. Troyanovskaya, *Bull. Acad. Sci. USSR, Div. Chem. Sci.*, 1971, **20**, 2497.
- 34 H. C. Brown, Y. M. Choi, and S. Narasimhan, *Inorg. Chem.*, 1981, **20**, 4454.
- 35 H. I. Schlesinger, H. C. Brown, H. R. Hoekstra and L. R. Rapp, *J. Am. Chem. Soc.*, 1953, **75**, 199.
- 10 36 M. H. Jones, W. Levason, C. A. McAuliffe and M. J. Parrott, *J. Chem. Soc. Dalton Trans.*, 1976, 1642.
- 37 V. A. Abakshin, G. A. Krestov and O. V. Eliseeva, *J. Gen. Chem. USSR*, 1987, **57**, 1431.
- 15 38 A. V. Levkin and A. Y. Tsivadse, *Russ. J. Inorg. Chem.*, 1986, **31**, 161.
- 39 B. D. James and M. G. H. Wallbridge, *Progr. Inorg. Chem.*, 1970, **11**, 99.
- 40 D. Seebach, A. Thaler and A. K. Beck, *Helv. Chim. Acta*, 1989, **72**, 857.
- 20 41 L. Banfi, E. Narisano, R. Riva and E. W. Baxter, *e-EROS Encycl. Reagents Org. Synth.*, **2005**.
- 42 U. Mirsaidov, A. Kurbobekov and M. Khikmatov, *Russ. J. Inorg. Chem.*, 1981, **26**, 1538.
- 25 43 V. D. Makhaev and K. N. Semenenko, *Bull. Acad. Sci. USSR Div. Chem. Sci.*, 1978, **27**, 2520.
- 44 V. D. Makhaev, A. P. Borisov, N. G. Mozgina, G. N. Boyko and K. N. Semenenko, *Neorg. Mater. (Inorg. Mater.)*, 1978, **14**, 1726.
- 45 45 R. Černý, G. Severa, D. B. Ravnsbæk, Y. Filinchuk, V. D'Anna, H. Hagemann, D. Haase, C. M. Jensen and T. R. Jensen, *J. Phys. Chem. C*, 2010, **114**, 1357.
- 30 46 D. B. Ravnsbæk, L.H. Sørensen, Y. Filinchuk, F. Besenbacher and T. R. Jensen, *Angew. Chem. Int. Ed.*, 2012, **51**, 3582.
- 47 T. Jaroń and W. Grochala, *Dalton Trans.*, 2010, **39**, 160.
- 35 48 T. Jaroń, W. Koźmiński and W. Grochala, *Phys. Chem. Chem. Phys.*, 2011, **13**, 8847.
- 49 T. Jaroń and W. Grochala, *Dalton Trans.*, 2011, **40**, 12808.
- 50 T. Jaroń, W. Wegner and W. Grochala, *Dalton Trans.*, 2013, **42**, 6886.
- 40 51 P. Panissod and M. Drillon in *Magnetism: Molecules to Materials IV: Nanosized Magnetic Materials*, ed. J. S. Miller and M. Drillon, Wiley-VCH Verlag GmbH, Weinheim, 2003, p. 243.
- 52 R. Liu, D. Reed and D. Book, *J. Alloys Compd.*, 2012, **515**, 32.
- 53 A. W. Addison, R. T. Nageswara, J. Reedijk, J. van Rijn and G. C. Verschoor, *J. Chem. Soc. Dalton Trans.*, 1984, 1349.
- 45 54 M. J. Ingleson, J. P. Barrio, J. Bacsá, A. Steiner, G. R. Darling, J. T. A. Jones, Y. Z. Khimiyak and M. J. Rosseinsky, *Angew. Chem. Int. Ed.*, 2009, **48**, 2012.
- 55 Agilent Technologies. CrysAlis PRO, 2013.
- 50 56 G. M. Sheldrick, *Acta Crystallogr. A.*, 2008, **64**, 112.
- 57 A. P. Hammersley, S. O. Svensson, M. Hanfland, A. N. Fitch and D. Hausermann, *High Press. Res.*, 1996, **14**, 235.
- 58 A. Boulfif and D. Louër, *J. Appl. Crystallogr.*, 2004, **37**, 724.
- 59 V. Favre-Nicolin and R. Černý, *J. Appl. Crystallogr.*, 2002, **35**, 734.
- 55 60 J. Rodríguez-Carvajal, *Phys. B Condens. Matter*, 1993, **192**, 55.
- 61 G. Kresse and J. Furthmüller, *Phys Rev B*, 1996, **54**, 11169.
- 62 P. E. Blöchl, *Phys. Rev. B* 1994, **50**, 17953.
- 63 J. P. Perdew, K. Burke and M. Ernzerhof, *Phys. Rev. Lett.*, 1996, **77**, 3865.
- 60 64 S. L. Dudarev, G. A. Botton, S. Y. Savrasov, C. J. Humphreys and A. P. Sutton, *Phys. Rev. B*, 1998, **57**, 1505.
- 65 C. Franchini, R. Podloucky, J. Paier, M. Marsman and G. Kresse, *Phys. Rev. B*, 2007, **75**, 195128.



41x20mm (600 x 600 DPI)